Texturing of String Ribbon Silicon

S. Gindner, J. Junge, S. Seren, G. Hahn
University of Konstanz, Department of Physics, Jacob-Burckhardt-Str. 29, 78464 Konstanz, Germany
Email: sarah.gindner@uni-konstanz.de, phone: +49-7531-882132, fax: +49-7531-883895

ABSTRACT: Surface texturing is a common way to enhance the amount of photons absorbed in a material by reducing reflectance and thus can be used to increase the short circuit current of a silicon solar cell. In this work a new promising one-sided wet chemical texture and an optimized SF_6/O_2 plasma texture are tested on String Ribbon (SR) material. For both textures reflectance measurements are presented and compared to monocrystalline FZ material which is used as reference. Solar cells are produced in a photolithography based high efficiency process. First cell results from plasma textured and non-textured wafers are obtained.
Keywords: Wet chemical texture, Plasma texture, ribbon silicon

1 INTRODUCTION

In this paper texturing of String Ribbon material as well as monocrystalline FZ material is investigated. String Ribbon is a special type of so called silicon ribbon material [1]. There are different ways to produce these ribbon wafers. One is pulling the material vertically out of the melt during crystallization [2] so that wafers only need to be cut afterwards. EFG (Edge Defined Film Fed Growth) and SR (String Ribbon) are representatives of this production method and the latter is analyzed here. Two different textures are applied. Since the production method induces no saw damage on vertically pulled ribbon wafers, most acidic textures do not deliver satisfying results like in the case for standard wire-sawn multicrystalline silicon[3]. Hence alternative ways for texturing of ribbon silicon are investigated. In the present work two different textures are compared. One is a new promising one-sided wet-chemical texture, the other one is a plasma texture based on SF_6 and O_2.

2 EXPERIMENTAL SET-UP

2.1 Process

Figure 1 shows the applied processing sequence [4] for lab-type solar cells. Full sized wafers are cut by a laser and cleaned by a polishing etch consisting of HF, HNO_3 and CH_3COOH. Afterwards some wafers are textured by SF_6/O_2 plasma or by the wet chemical etch [5] while adjacent wafers of similar grain structure remain untextured for comparison. Both textures leave the rear side untextured. The emitter diffusion is carried out in an industrial-type $POCl_3$ diffusion furnace. The following step is a PECVD (Plasma Enhanced Chemical Vapor Deposition) SiN_x:H deposition for front surface passivation and as anti reflection coating. For backside passivation a conventional Al paste is screen-printed on the rear, then dried and fired in a conventional belt furnace to form the Al-BSF. During the firing step hydrogen is released from the SiN_x:H layer to passivate bulk defects. After wet chemical etching of the Al paste, the front contacts are defined by photolithography and evaporation of Ti, Pd and Ag followed by Ag plating. Al for the rear contact is also evaporated. Finally four solar cells (format 2 x 2 cm²) are cut out of each 5 x 5 cm² wafer with a dicing saw. A MIRHP (Microwave-Induced Remote Hydrogen Plasma) step for contact sintering and low temperature hydrogenation (< 400°C) finalizes the process. After IV characterization a Double Anti Reflection Coating (DARC) of MgF_2 of about 110 nm in thickness is evaporated on the best cells in order to additionally increase the short circuit current.

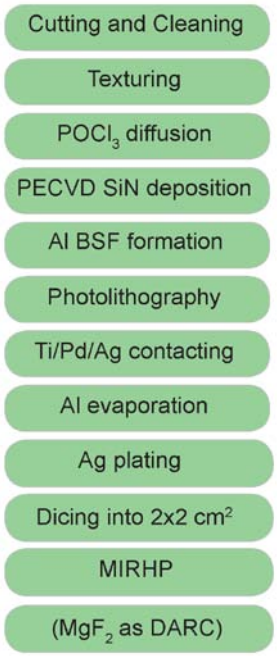

Figure 1: Processing sequence for the applied high efficiency cell process including the plasma texture.

2.2 Investigated material

The investigated SR material has long grains which typically extend over a few 8 x 15 cm^2 wafers and can be around 1 cm wide. The typical base resistance is about 2-4 Ωcm. Wafers for the experiment are selected so that three 5 x 5 cm^2 wafers cut out of a 8 x 15 cm² wafer have a similar grain structure (adjacent wafers, ID A, B, C) to facilitate comparison of the different textures. Non-textured wafers are processed within the same experiments to demonstrate the difference between flat and textured wafer surfaces. As reference material 0.5 Ωcm FZ is used.

3 RESULTS

3.1 Comparison of the two different textures

The wet chemical texture is analyzed and compared to the plasma texture, which is already optimized for ribbon silicon at UKN [6]. In comparison, the wet chemical texture is not yet optimized and lower reflectivities are expected in future experiments. In Figure 4 reflectance measurements of three comparable SR and FZ wafers are shown. All textured wafers show a significant reduction of reflectivity. Especially the curves of FZ material match each other closely. In the case of SR material, reflectance of the plasma texture is slightly lower than the one of the wet chemical texture in the wavelength region between 350 and 1000 nm. For better comparison reflection coefficients at 700 nm are given in Table I.

Table I: Reflection at 700 nm depicted from Figure 4.

Material	R_non-textured (%)	R_plasma (%)	R_wet chemical (%)
FZ	33.4	18.9	18.4
SR	33.5	18.7	22.5

The SR wafer with plasma texture exhibits a reflectivity of 18.7%. The wet chemically textured SR wafer shows a slightly higher value of 22.5%.

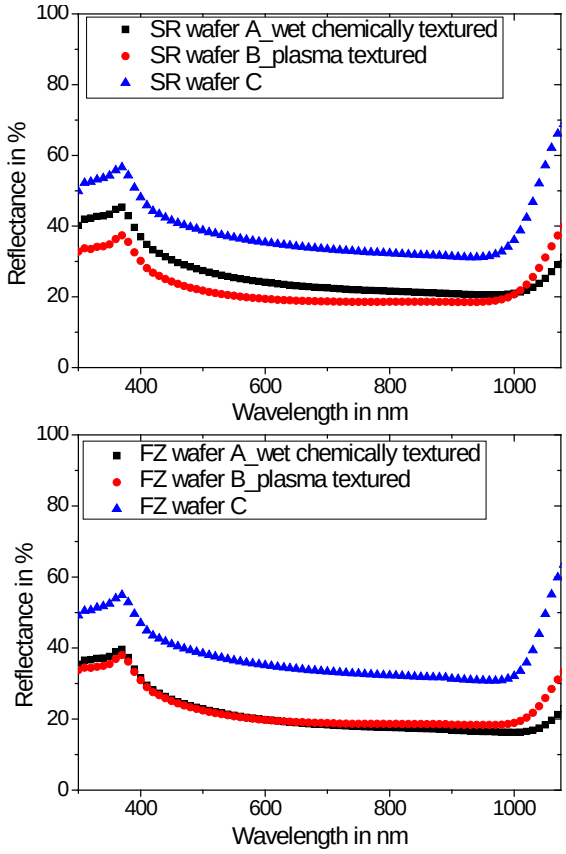

Figure 4: Reflectance data of three comparable SR and FZ wafers A, B, C with varying surface treatment.

In comparison to the non-textured wafer, that corresponds to a relative reduction by 44% in case of the plasma texture and 33% for the wet chemically treated material.

Figure 5 shows SEM images of a wet chemical texture (left) and a plasma texture (right) on SR material. Two grain boundaries within the wet chemical texture can be seen in both upper images on the left. The texture successfully crosses the grain boundaries with minor variations in the pit shapes along the grain boundary and from grain to grain. The plasma texture forms a sponge-like structure on the wafer surface with cavities of different sizes up to a diameter of 0.5 µm. In contrast to that, the wet chemical etching results in a very periodical honeycomb surface pattern consisting of bowl-shaped structures with ~20 µm in diameter.

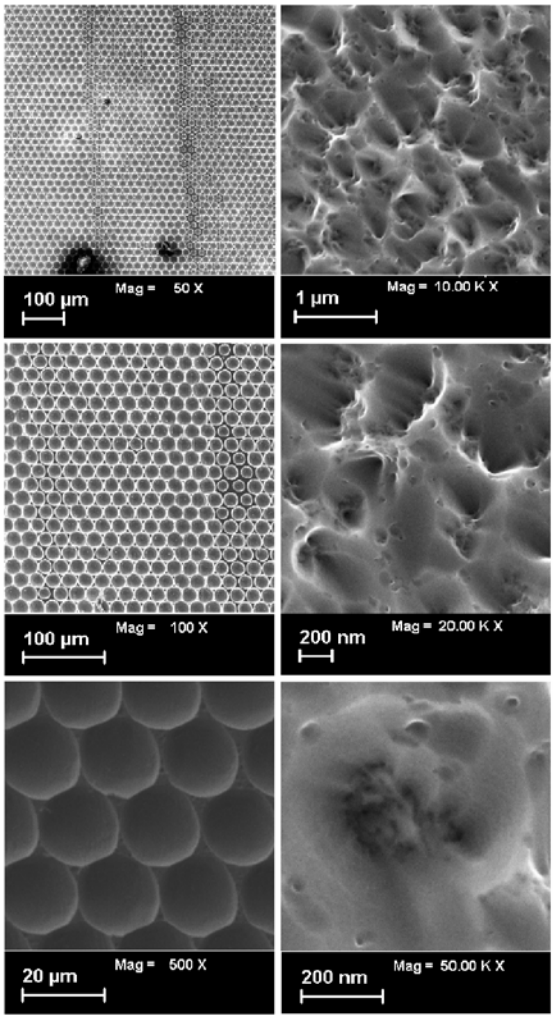

Figure 5: SEM images of the wet chemical texture (left) and the plasma texture (right) on SR material.

3.2 First cell results

The cell process shown in Figure 1 is carried out on non-textured and plasma textured SR and FZ material. Cell runs including wet chemically textured wafers are still on schedule. The results of the best produced solar cells are depicted in Table II. Fill factors of nearly 80% could be obtained. Via the plasma texturing the short circuit current density of the cells could be raised by 1.4 mA/cm^2 for String Ribbon and by 1.5 mA/cm^2 for the

FZ references. Unfortunately, the reduction of V_{oc} from

Table II: IV data of SR and FZ solar cells. Cells shown in 2 are highlighted according to their line color.

Material	FF [%]	j_{SC} [mA/cm^2]	V_{OC} [mV]	η [%]	j_{01} [10^{-13} A/cm^2]	j_{02} [10^{-8} A/cm^2]
SR_untex	79.6	33.1	628.2	16.5	6.8	2.3
SR_tex	79.2	34.5	612.5	16.7	13	2.8
FZ_untex	80.6	33.2	644.3	17.2	3.7	1.3
FZ_tex	79.1	34.7	640.4	17.6	3.9	2.7

628 mV to 612 mV due to the plasma texture is rather high for the SR material whereas the FZ material seems much less affected by the roughened front surface. A detailed analysis of measured IV curves leads to the saturation current j_{01} which is the first term in the two diode model. It takes into account the recombination losses within emitter and base. If there is more recombination the saturation current is raised while voltage is lowered. The reduction in V_{oc} for String Ribbon is accompanied by the increase of $j_{01,untext} = 6.8\ 10^{-13}$ A/cm^2 up to $j_{01,text} = 1.3\ 10^{-12}$ A/cm^2. There can be two explanations for that. One is that the plasma texture influences bulk lifetime, which is not approved by former processes. The second one is more likely and is discussed later on: Inhomogeneities of Al-BSF layer could have led to varying backside passivation from cell to cell. Since no change in j_{02} due to plasma texturing is observable, it can be assumed that the space charge region is not affected by recombination losses. j_{01} and j_{02} of FZ material almost remain unchanged after texturing which means no recombination. It should be mentioned, however, that bulk lifetime within emitter and base could also be limited by defects in case of String Ribbon.

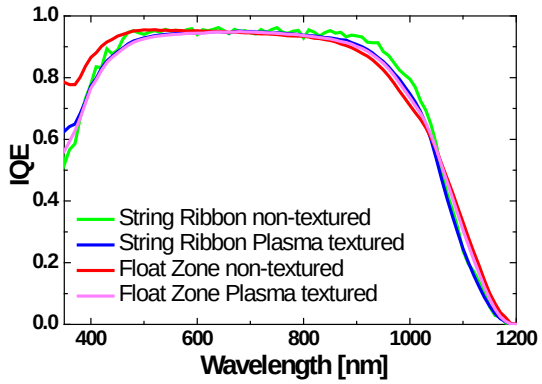

Figure 2: Internal quantum efficiency curves of plasma textured and non-textured SR and FZ material.

As can be seen from the IQE data in Figure 2, the long wavelength IQE is very similar for all cells presented. This indicates that the bulk lifetime is not limiting the cell performance, but the cell process including a full Al-BSF is the limiting factor. In the short wavelength region a rather low IQE for values around 400 nm can be observed. This indicates that the applied emitter is not yet fully optimized. The fact, that the blue response is higher for untextured cells, can be explained by the larger surface area of the plasma texture which is more difficult to passivate. A higher quality emitter would therefore lead to a better blue response and therefore higher j_{sc} values. The fact that the untextured FZ cell shows a significantly higher IQE is probably due to better passivation of the non-textured surface. Similar behavior has been observed before for plasma textured cells, and the fact that this phenomenon does not show up clearly for the untextured String Ribbon cell might be due to problems with the vacuum chuck during the IQE measurement.

The long wavelength IQE values of FZ cells only reach about 70% at 1000 nm, which is quite low for the used 0.5 Ωcm material. This may be explained by the thickness of the Al–BSF (Aluminum Back Surface Field). Figure 3 shows that the ECV (Electrochemical Capacitance Voltage) profile of the Al-BSF from a FZ solar cell originating from a prior process is nearly twice as thick as the Al-BSF from a recent FZ sample. This is most probably caused by an insufficient amount of Al paste on the wafers and/or by a firing temperature that was chosen too low. Both will be optimized for further cell processes.

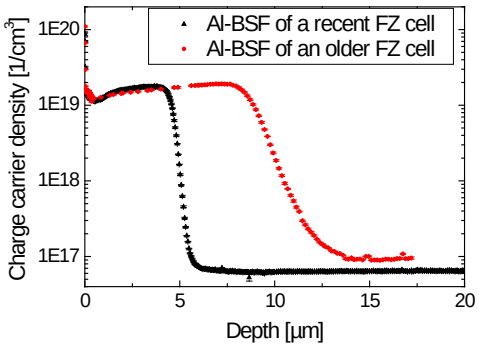

Figure 3: ECV profile of an Al-BSF from a FZ cell out of the recent process (black) compared to a FZ cell out of a foregoing process (red).

By applying a DARC (Double Anti Reflection Coating) even higher efficiencies could be reached. The short circuit current density is raised by about 1 mA/cm^2 on the textured samples. Non-textured samples profit even more from the DARC because the relative decrease of the reflectance on a flat surface is higher. This could be of industrial relevance since the module glass and encapsulatn act similar to a second layer anti-reflection coating. Results are given in Table III.

Table III: IV data of SR and FZ cells with DARC. Cells shown in Figure 2 are highlighted according to their line color.

Material	FF [%]	j_{SC} [mA/cm^2]	V_{OC} [mV]	η [%]	j_{01} [10^{-13} A/cm^2]	j_{02} [10^{-8} A/cm^2]
SR_untex	79.6	34.9	630.2	17.5	6.5	2.7
SR_tex	79.4	35.5	613.3	17.3	14	3.75
FZ_untex	80.5	34.7	645.6	18.1	3.7	1.27
FZ_tex	79.5	35.9	641.4	18.3	4.1	2.3

4 SUMMARY AND OUTLOOK

Due to texturing, the reflectivity of SR material could be reduced successfully by 33% rel. in case of wet chemical texturing and 44% rel. for plasma texture, respectively.

Non-textured String Ribbon cells reached efficiencies up to 16.5% and plasma textured solar cells processed from adjacent wafers 16.7%. Non-textured FZ material resulted in an efficiency up to 17.2% and textured FZ up to 17.6% (all cells with SARC).

Although a gain in j_{SC} is observable as expected, V_{OC} is significantly decreased on plasma textured SR solar cells.

By applying an additional DARC layer the difference in short circuit current density between plasma textured and non-textured solar cells decreased again.

A comparison between wet chemical and plasma textured cells will be performed in the future.

5 ACKNOWLEDGEMENTS

We would like to thank A. Dastgheib-Shirazi for advice and help during processing. For technical support we thank B. Rettenmaier, L. Rothengaß and J. Ruck.

6 REFERENCES

[1] G. Hahn and A. Schönecker "*New crystalline silicon ribbon materials for photovoltaics*", J. Phys. Condens. Matter

[2] F. Wald, *Crystals: Growth, Properties and Applications* 5, Springer, 1981.

[3] G. Hahn, I. Melnyk, C. Dube, and A.M. Gabor, "*Development of a Chemical Surface Texture for String Ribbon Silicon Solar Cells"*, Proceedings of the 20th EC PVSEC, Barcelona, 2005

[4] J. Junge et al. *"Advanced Processing Steps For High Efficiency Solar Cell Based On EFG Material"*, Proc. 33rd IEEE PVSC, San Diego, 2008

[5] E. M. Sachs al, "*1366-Texture and 1366-Metallization: Superior Light Trapping and 30-Micron Fingers for Any Silicon Wafer Type at Low Cost*", Proc. 25th EU PVSEC, Valencia

[6] D. Groetschel et al. *"Plasma Texturing and its influence on surface passivation"*, 23rd EU PVSEC Valencia, 2008